

Strange molecular partners of the $Z_c(3900)$ and $Z_c(4020)$

Zhi Yang,^{1,*} Xu Cao,^{2,3,†} Feng-Kun Guo,^{4,3,‡} Juan Nieves,^{5,§} and Manuel Pavon Valderrama^{6,¶}

¹*School of Physics, University of Electronic Science and Technology of China, Chengdu 610054, China*

²*Institute of Modern Physics, Chinese Academy of Sciences, Lanzhou 730000, China*

³*University of Chinese Academy of Sciences, Beijing 100049, China*

⁴*CAS Key Laboratory of Theoretical Physics, Institute of Theoretical Physics, Chinese Academy of Sciences, Beijing 100190, China*

⁵*Instituto de Física Corpuscular (centro mixto CSIC-UV), Institutos de Investigación de Paterna, Apartado 22085, 46071, Valencia, Spain*

⁶*School of Physics and Nuclear Energy Engineering, International Research Center for Nuclei and Particles in the Cosmos and Beijing Key Laboratory of Advanced Nuclear Materials and Physics, Beihang University, Beijing 100191, China*

(Dated: September 11, 2022)

Quantum Chromodynamics presents a series of exact and approximate symmetries which can be exploited to predict new hadrons from previously known ones. The $Z_c(3900)$ and $Z_c(4020)$ resonances, which have been theorized to be isovector $D^*\bar{D}$ and $D^*\bar{D}^*$ molecules [$I^G(J^{PC}) = 1^-(1^{+-})$], are no exception. Here we argue that from SU(3)-flavor symmetry, we should expect the existence of strange partners of the Z_c 's with hadronic molecular configurations $D^*\bar{D}_s-D\bar{D}_s^*$ and $D^*\bar{D}_s^*$ (or, equivalently, quark content $c\bar{c}s\bar{q}$, with $q = u, d$). The quantum numbers of these Z_{cs} and Z_{cs}^* resonances would be $I(J^P) = \frac{1}{2}(1^+)$. The predicted masses of these partners depend on the details of the theoretical scheme used, but they should be around the $D^*\bar{D}_s-D\bar{D}_s^*$ and $D^*\bar{D}_s^*$ thresholds, respectively. We show that, together with a possible triangle singularity contribution, such a picture nicely agrees with the very recent BESIII data of the $e^+e^- \rightarrow K^+(D_s^- D^{*0} + D_s^{*-} D^0)$.

Introduction.— Unsuccessful searches for charged charmonium-like states ($Z_{cs}^{(*)}$) with hidden-charm and open-strange channels in $e^+e^- \rightarrow K^+K^-J/\psi$ have been in the past reported by Belle [1, 2] and BESIII [3]. Recently, however, the BESIII collaboration has observed [4] a new strange, hidden-charm resonance with a mass and width of

$$M(Z_{cs}) = 3982.5_{-2.6}^{+1.8} \pm 2.1 \text{ MeV}, \quad (1)$$

$$\Gamma(Z_{cs}) = 12.8_{-4.4}^{+5.3} \pm 3.0 \text{ MeV}. \quad (2)$$

This raises the question of what its nature is. Its closeness to the two-meson $D^*\bar{D}_s-D\bar{D}_s^*$ thresholds immediately suggests the possibility that it might be a hadronic molecule. Theoretical predictions of Z_{cs} states have been made in different models [5–7], and in general lie much more above the $D\bar{D}_s^*/D^*\bar{D}_s$ and $D^*\bar{D}_s^*/\bar{D}^*D_s^*$ thresholds than what can be inferred from the new BESIII results. The only exception is the QCD sum rule study of Ref. [5], where a $D_s\bar{D}^* + D_s^*\bar{D}$ molecule with $J^P = 1^+$ and mass 3.96 ± 0.10 GeV is obtained. And in Ref. [8], cusps were predicted at the $D_s^{(*)}D^*$ thresholds in the $J/\psi K$ distribution.

To evaluate the reliability of the hadronic molecular hypothesis it is interesting to compare the new $Z_{cs}^{(*)}$ resonance with other known molecular candidates. Of particular relevance is the previous discovery by BESIII [9, 10] of the $Z_c(3900)$ and $Z_c(4020)$ (Z_c and Z_c^* from now on), two charged hidden charm states located very close to the $D\bar{D}^*$ and $D^*\bar{D}^*$ thresholds, respectively (as can be checked in the review of particle physics (RPP) [11]),

suggesting a molecular nature of the Z_c and Z_c^* . Going further back in time, a decade ago the Belle collaboration discovered the $Z_b(10610)$ and $Z_b(10650)$ (Z_b and Z_b^*), a pair of charged hidden-bottom resonances with $I^G(J^{PC}) = 1^-(1^{+-})$ and masses also very close to the $B\bar{B}^*$ and $B^*\bar{B}^*$ thresholds [12], which raised the question whether the Z_b 's were indeed bound states of the bottom mesons mentioned above.

Symmetries.— The fact that the Z_c 's and Z_b 's come in pairs is naturally explained within the molecular picture from heavy-quark spin symmetry (HQSS) considerations. This happens when the off-diagonal piece between the $D\bar{D}^*(B\bar{B}^*)$ and $D^*\bar{D}^*(B^*\bar{B}^*)$ is neglected. Such a phenomenon was called by Voloshin as “light-quark spin symmetry” [13], and the experimental observations are consistent with such a picture. In addition, the existence of the hidden-charm pair can be deduced from the hidden-bottom one and the heavy-flavor symmetry (HFS) for the potential [14], though whether the relation between the hidden charm and bottom sectors is of a phenomenological or systematic nature has recently been challenged [15]. The question we would like to address in this work is whether the new Z_{cs} resonance is related to the Z_c and Z_c^* .

Besides heavy quarks, the $Z_c^{(*)}$'s also contain light quarks, which means that they are constrained by the usual SU(2)-isospin and SU(3)-flavor symmetries (possible consequences of these symmetries have been explored in [16, 17]). If we generically denote the $D^{(*)}$ and $D_s^{(*)}$ mesons as $D_a^{(*)}$, with the subindex a denoting flavor, it

happens that the $D_a^{(*)}$ mesons belong to the $\bar{3}$ representation of SU(3). From this we deduce that the $D_a^{(*)}\bar{D}^{(*)a}$ system will be a combination of the $3\otimes\bar{3} = 1\oplus 8$ representations, i.e., a combination of a singlet and an octet. The flavor structure of the $D_a^{(*)}\bar{D}^{(*)a}$ potential, in a given J^P sector with definite C -parity for the flavor neutral states, will be

$$V = \lambda_S V^{(S)} + \lambda_O V^{(O)}, \quad (3)$$

with $V^{(S)}$ and $V^{(O)}$ denoting the singlet and octet parts of the potential, which are related to the parameters $C_{0A,0B}$ and $C_{1A,1B}$ in Ref. [16] as $V^{(O)} = (C_{1A} - C_{1B})$ and $V^{(S)} = (C_{0A} - C_{0B})$. For the $D^{(*)}\bar{D}^{(*)}$ system the potential will be

$$V(D^{(*)}\bar{D}^{(*)}, I=0) = \frac{2}{3}V^{(S)} + \frac{1}{3}V^{(O)}, \quad (4)$$

$$V(D^{(*)}\bar{D}^{(*)}, I=1) = V^{(O)}, \quad (5)$$

depending on whether we have an isoscalar or isovector meson-antimeson pair. For the $D^{(*)}\bar{D}_s^{(*)}$ system we have a pure octet configuration

$$V(D^{(*)}\bar{D}_s^{(*)}, I=1) = V^{(O)}, \quad (6)$$

while for the $D_s^{(*)}\bar{D}_s^{(*)}$ system we obtain

$$V(D_s^{(*)}\bar{D}_s^{(*)}, I=0) = \frac{1}{3}V^{(S)} + \frac{2}{3}V^{(O)}. \quad (7)$$

Of course, SU(3)-flavor symmetry is not exact, and we expect these relations to be violated at about a 20% level.

Now, if we notice that the odd C -parity Z_c^0 is in an octet configuration, the potential for a prospective $D^*\bar{D}_s$ and $D^*\bar{D}_s^*$ $I(J^P) = 1/2(1^+)$ molecule will be identical to that of the strangeless Z_c 's. This implies the existence of Z_{cs} and Z_{cs}^* partners of the $Z_c(3900)$ and $Z_c^*(4020)$. The predictions for the masses of these states will depend on the details of the potential, but we can make a first approximation by assuming that the charmed mesons are massive enough as to ignore the kinetic energy term in the Schrödinger equation

$$H = T_{\text{kin}} + V \approx V \quad (\text{for } m_{D_a}, m_{D_a^*} \rightarrow \infty), \quad (8)$$

in which case the binding energy of the molecule will be given by the matrix element of the potential, i.e. $E_B \simeq \langle V \rangle$. Within this approximation, one would find

$$M(Z_c^*) - 2m_{D^*} \simeq M(Z_{cs}^*) - (m_{D^*} + m_{D_s^*}), \quad (9)$$

plus analogous relations for the Z_c and Z_{cs} states. This will translate into predicted masses of around 3.99 GeV and 4.13 GeV for the Z_{cs} and Z_{cs}^* resonances, respectively.

EFT description.— This simple approximation is not expected to be particularly accurate for the charmed mesons, at least at first sight. If we want to check its

correctness, or improve over it, we propose a concrete form for the potential. The most general way to derive the interaction is from an effective field theory (EFT). In particular if we use a pionless EFT or a pionful EFT where pions are perturbative [18], the lowest order EFT potential we will obtain is simply a contact-range interaction without derivatives

$$V_{\text{virtual}}^{(O)} = C^{(O)}. \quad (10)$$

This interaction is able to generate a pole below its respective two-meson threshold (a bound or a virtual state), but not above the threshold. This is what might be happening in the Z_c and Z_c^* cases, whose Breit-Wigner (BW) masses are around 11 and 7 MeV above their respective thresholds, though it is perfectly possible that the BW parametrization used to determine these masses could not correspond to their physical poles, which could very well be below threshold [19]. Alternatively we can use a different EFT suited for a resonant state, where the contact-range potential will take the form

$$V_{\text{res}}^{(O)} = C^{(O)} + 2D^{(O)}k^2, \quad (11)$$

with k the c.m. momentum of the two mesons, and where the two low-energy constants (LECs) $C^{(O)}$ and $D^{(O)}$ can be directly determined from the Z_c and Z_c^* masses and widths.

To make predictions for the Z_{cs} with the previous interactions, first we have to determine the LECs from the Z_c/Z_c^* poles. We will use the virtual-state and resonant Z_c pole positions extracted in Ref. [19] as inputs. Note that the Z_c/Z_c^* masses and widths given in RPP are not from a pole analysis and not well suited for our purpose. In addition, the virtual and resonant EFT potentials have to be regularized, included in a dynamical equation to obtain the poles and then renormalized. For the regularization we will use a Gaussian regulator of the type

$$\langle p' | V_{\Lambda}^{(O)} | p \rangle = V^{(O)} g\left(\frac{p'}{\Lambda}\right) g\left(\frac{p}{\Lambda}\right), \quad (12)$$

with $g(x) = e^{-x^2}$ and $V^{(O)}$ the unregularized potential of Eqs. (10) or (11), where the couplings now depend on the cutoff, i.e., $C^{(O)} = C^{(O)}(\Lambda)$ and $D^{(O)} = D^{(O)}(\Lambda)$.

For the dynamical equation we will consider the Lippmann-Schwinger equation — $T = V + VG_0T$ — which for a separable potential admits the ansatz

$$\langle p' | T(E_{\text{cm}}) | p \rangle = \tau(E_{\text{cm}}) g\left(\frac{p'}{\Lambda}\right) g\left(\frac{p}{\Lambda}\right) \quad (13)$$

where $\tau(E_{\text{cm}})$ is given by

$$\frac{1}{\tau(E_{\text{cm}})} = \frac{1}{C^{(O)} + 2D^{(O)}k^2} - I_0(E_{\text{cm}}; \Lambda), \quad (14)$$

with the loop integral

$$I_0(E_{\text{cm}}; \Lambda) = \int \frac{d^3q}{(2\pi)^3} \frac{g^2\left(\frac{q}{\Lambda}\right)}{E_{\text{cm}} - M_{\text{th}} - \frac{q^2}{2\mu} + i\epsilon}, \quad (15)$$

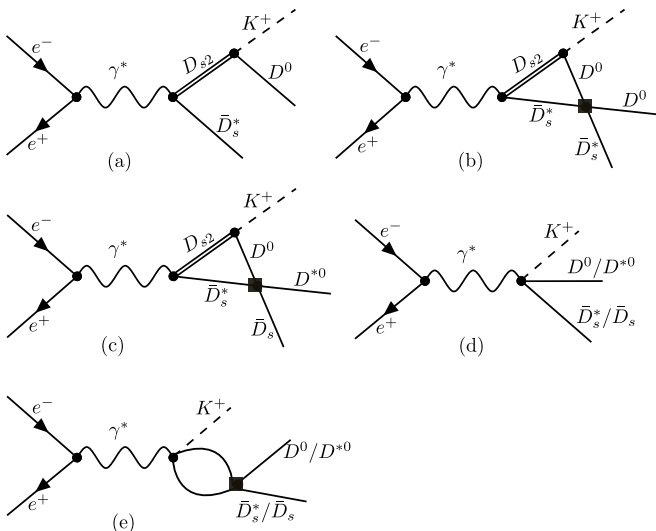


FIG. 1. Feynman diagrams for the production mechanisms considered in this work: (a) and (b) for the $K^+ D_s^* \bar{D}^0$; (c) for the $K^+ D_s \bar{D}^{*0}$; (d) and (e) for both final states. The filled squares denote the T -matrix elements which include the effects of the generated Z_{cs} state.

where E_{cm} is the c.m. energy of the two-body system (if above threshold $E_{\text{cm}} = M_{\text{th}} + k^2/2\mu$), $M_{\text{th}} = m_1 + m_2$ and $\mu = m_1 m_2 / (m_1 + m_2)$, with m_1, m_2 the meson masses. The $Z_c^{(*)}$ and $Z_{cs}^{(*)}$ states correspond to poles of the T -matrix, i.e. to $1/\tau(E_{\text{pole}}) = 0$, in appropriate Riemann sheets. Finally, we notice that for the Z_{cs} state there is the subtlety of the existence of two nearby thresholds with slightly different masses: $D \bar{D}_s^*$ and $D^* \bar{D}_s$. Yet the energy gap between the two thresholds is merely 2.5 MeV. For this reason we will simply take the approximation that the two thresholds are at the same energy, for which we will take the average of the two channels.

Determination of the LECs (previous data)— For the determination of the couplings, first we fit to the location of the Z_c and Z_c^* poles as extracted in Ref. [19]. In the *constant-contact* EFT without the $D^{(O)}$ term, we obtain for $\Lambda = 0.5(1.0)$ GeV

$$C^{(O)}(\Lambda) = -0.29_{-0.32}^{+0.15} (-0.28_{-0.39}^{+0.08}) \text{ fm}^2, \quad (16)$$

while for the *resonant* EFT with both the $C^{(O)}$ and $D^{(O)}$ terms, we find

$$\begin{aligned} C^{(O)}(\Lambda) &= -0.06_{-0.16}^{+0.24} (-0.22_{-0.06}^{+0.10}) \text{ fm}^2, \\ D^{(O)}(\Lambda) &= -0.31_{-0.17}^{+0.10} (-0.09_{-0.07}^{+0.03}) \text{ fm}^4, \end{aligned} \quad (17)$$

with errors added in quadrature. The predictions for the Z_{cs} 's spectrum with this method are summarized in the upper half of Table I.

Analysis of the new data.— The new measurements of the $e^+e^- \rightarrow K^+(D_s^* \bar{D}^0 + D_s \bar{D}^{*0})$ data from 4.628–4.698 GeV also allow us to determine the LECs from an independent source. For this process one readily

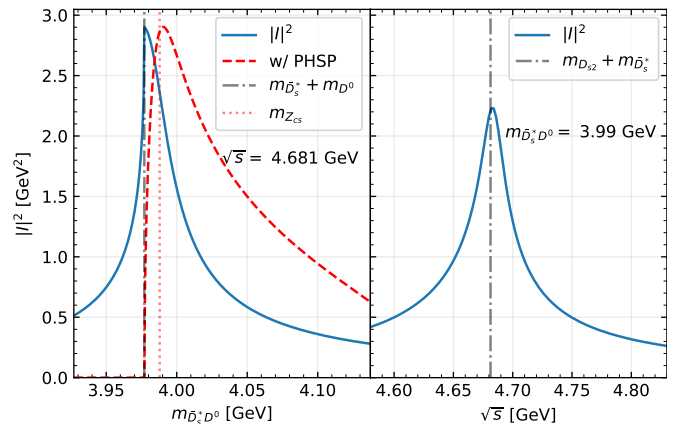


FIG. 2. Absolute squared value of the scalar triangle loop integral, $|I|^2$, with the $D_{s2} \bar{D}_s^* D^0$ intermediate state shown as Fig. 1(b). Left: dependence on the $\bar{D}_s^* D^0$ invariant mass for $\sqrt{s} = 4.68$ GeV, where we also show $|I|^2$ convolved with the phase space, with the maximum normalized to that of $|I|^2$; right: dependence on \sqrt{s} with $m_{\bar{D}_s^* D^0} = 3.99$ GeV.

notices that there are triangle diagrams shown as diagrams (b) and (c) in Fig. 1. The triangle diagrams are special in the sense that they possess a triangle singularity [20] when the e^+e^- c.m. energy is around the $D_{s2} \bar{D}_s^*$ threshold at 4.681 GeV. A triangle singularity happens when all the intermediate particles in a triangle diagram are on their mass shell and move collinearly so that the whole process may be regarded as a classical process in the spacetime [21]. Although triangle singularities have been known for a long time, no clear signal has been observed until recent years when many new resonant hadronic structures were reported in various high-energy experiments. A review of the effects of triangle singularities in the context of exotic hadrons can be found in Ref. [22]. On the one hand, triangle singularities produce peaks mimicking the resonance behavior; on the other hand, they can enhance the production of near-threshold hadronic molecules as emphasized in Refs. [22, 23]. For instance, the importance of the $D_1(2420) \bar{D} D^*$ triangle diagrams for the Z_c structures is discussed in Refs. [19, 24–28]. Here, one finds that the production of the Z_{cs} can be facilitated by the $D_{s2} \bar{D}_s^* D^0$ triangle diagrams shown in Fig. 1. To see this clearly, we show the absolute value squared of the corresponding scalar triangle loop integral, $|I|^2$, in Fig. 2. In the left panel, we also show $|I|^2$ convolved with the three-body phase space for $e^+e^- \rightarrow K^+ \bar{D}_s^* D^0$ with $\sqrt{s} = 4.68$ GeV, which clearly presents a peak around 3.99 GeV. Thus, such an effect needs to be taken into account when extracting information of Z_{cs} from the data. The expression for I can be found in Refs. [22, 23, 29]. To account for the finite width, 16.9 MeV, of the $D_{s2}(2573)$, we use a complex value $(2569.1 - i8.5)$ MeV [11] as its mass.

The amplitudes corresponding to the diagrams shown

TABLE I. Pole positions (MeV units) of even parity octet $D^{(*)a}\bar{D}_a^{(*)}$ molecules with $J^P = 1^+$. Non-strange states have $I^G = 1^-$ and negative charge-conjugation quantum numbers (for the neutral ones). For the numerical calculations, we have used $m_D = 1867.2$ MeV, $m_{D^*} = 2008.6$ MeV, $m_{D_s} = 1968.3$ MeV and $m_{D_s^*} = 2112.2$ MeV. We show results from both the constant-contact and resonant EFTs introduced in Eqs. (10) and (11). The LECs are determined in two ways, either by reproducing the position of the Z_c pole obtained in Ref. [19] (top first two sets of pole positions) or by directly fitting to the BESIII data of $e^+e^- \rightarrow K^+(D_s^- D^{*0} + D_s^{*-} D^0)$ [4] (bottom two sets). The values of $C^{(O)}$ and $D^{(O)}$ are given in Eqs. (16) and (17) in the former case, while those determined from the fits to data can be found in Eqs. (19) and (20), for the constant-contact and resonant EFTs (fits I and II, respectively). If there is no width, the pole corresponds to a virtual state solution. For fit II we have propagated the errors in quadrature, which might result in an overestimation of the uncertainties for the masses since we are not considering correlations. We note that this fit allows both for resonant (R) and virtual state (V) solutions. We find, in general, states significantly wider than in Eq. (2), which does not consider the triangle singularity and is based on a BW parametrization with an energy-dependent width instead.

Potential	States	Thresholds	Masses ($\Lambda = 0.5$ GeV)	Masses ($\Lambda = 1$ GeV)	Experiment
$V_{\text{virtual}}^{(O)}$	$\frac{1}{\sqrt{2}}(D\bar{D}^* - D^*\bar{D})$	3875.8	Input [19]	Input [19]	3888.4 ± 2.5 [11]
	$D^*\bar{D}^*$	4017.2	3988_{-27}^{+21}	3978_{-36}^{+25}	4024.1 ± 1.9 [11]
	$D\bar{D}_s^*/D^*\bar{D}_s$	3979.4/3976.9	3948_{-27}^{+22}	3937_{-36}^{+25}	
	$D^*\bar{D}_s^*$	4120.8	4092_{-26}^{+21}	4083_{-35}^{+24}	
Potential	States	Thresholds	Masses ($\Lambda = 0.5$ GeV)	Masses ($\Lambda = 1$ GeV)	Experiment
$V_{\text{res}}^{(O)}$	$\frac{1}{\sqrt{2}}(D\bar{D}^* - D^*\bar{D})$	3875.8	Input [19]	Input [19]	3888.4 ± 2.5 [11]
	$D^*\bar{D}^*$	4017.2	$4025 \pm 4 - i(21 \pm 7)$	$4035 \pm 6 - i(29 \pm 13)$	4024.1 ± 1.9 [11]
	$D\bar{D}_s^*/D^*\bar{D}_s$	3979.4/3976.9	$3986 \pm 4 - i(22 \pm 7)$	$3996 \pm 6 - i(30 \pm 13)$	$3982.5_{-3.3}^{+2.8} - i25.6_{-10.6}^{+12.1}$ [4]
	$D^*\bar{D}_s^*$	4120.8	$4129 \pm 4 - i(21 \pm 7)$	$4138 \pm 6 - i(28 \pm 12)$	
Potential	States	Thresholds	Masses ($\Lambda = 0.5$ GeV)	Masses ($\Lambda = 1$ GeV)	Experiment
$V_{\text{virtual}}^{(O)}$ [fit I, Eq. (19)]	$\frac{1}{\sqrt{2}}(D\bar{D}^* - D^*\bar{D})$	3875.8	3871_{-3}^{+2}	3867_{-7}^{+4}	3884.4 ± 2.5 [11]
	$D^*\bar{D}^*$	4017.2	4014_{-3}^{+2}	4012_{-6}^{+3}	4024.1 ± 1.9 [11]
	$D\bar{D}_s^*-D^*\bar{D}_s$	3979.4, 3976.9	3974_{-3}^{+2}	3971_{-6}^{+3}	
	$D^*\bar{D}_s^*$	4120.8	4117_{-5}^{+3}	4115_{-6}^{+3}	
Potential	States	Thresholds	Masses ($\Lambda = 0.5$ GeV)	Masses ($\Lambda = 1$ GeV)	Experiment
$V_{\text{res}}^{(O)}$ [fit II, Eq. (20)]	$\frac{1}{\sqrt{2}}(D\bar{D}^* - D^*\bar{D})$	3875.8	$3861_{-0}^{+20} - i6_{-6}^{+14}$ (R/V)	$3861_{-35}^{+16} - i0_{-0}^{+29}$ (R/V)	3884.4 ± 2.5 [11]
	$D^*\bar{D}^*$	4017.2	$4004_{-0}^{+18} - i0_{-0}^{+20}$ (R/V)	$4006_{-37}^{+10} - i0_{-0}^{+28}$ (R/V)	4024.1 ± 1.9 [11]
	$D\bar{D}_s^*-D^*\bar{D}_s$	3979.4, 3976.9	$3963_{-3}^{+20} - i3_{-3}^{+16}$ (R/V)	$3966_{-36}^{+12} - i0_{-0}^{+20}$ (R/V)	$3982.5_{-3.3}^{+2.8} - i25.6_{-10.6}^{+12.1}$ [4]
	$D^*\bar{D}_s^*$	4120.8	$4110_{-0}^{+14} - i0_{-0}^{+19}$ (R/V)	$4111_{-25}^{+9} - i0_{-0}^{+15}$ (R/V)	

in Fig. 1 can be easily worked out within the non-relativistic approximation for all the charmed mesons (for explicit expressions, we refer to the Appendix), which can be used to fit the invariant mass spectra measured by BESIII.

The BESIII data were collected at five c.m. e^+e^- energies ranging from 4.628 to 4.698 GeV. Since the data points have asymmetric Poisson upper and lower errors, we define χ^2 as

$$\chi^2 = \sum_i \frac{[f(x_i) - y_i]^2}{e_i^2} \quad (18)$$

with e_i chosen to be the lower error if $f(x_i) - y_i < 0$, and the upper error otherwise. We fit to the data up to 50 MeV above the threshold, i.e., 4.03 GeV. In this energy range, the nonrelativistic approximation for the charmed mesons work very well, and the c.m. momentum is at most 316 MeV, much smaller than the Gaussian cutoff

values that are used. The LECs $C^{(O)}$, $D^{(O)}$ entering the T -matrix in diagrams (b, c, e) can be extracted from the fit to the data. The other parameters include, for the event spectra at all the five e^+e^- energies, an overall normalization factor and a relative coupling strength for diagrams (d, e) in comparison with that of diagrams (a, b, c) in Fig. 1 ($\tilde{\mathcal{N}}$ and r in the appendix). In total, there are 4 free parameters. The fit is performed using the MINUIT function minimization and error analysis package [30–32].

For the constant-contact case, we find

$$C^{(O)}(\Lambda) = -0.77_{-0.10}^{+0.12} (-0.45_{-0.04}^{+0.05}) \text{ fm}^2, \quad (19)$$

with $\chi^2/\text{dof} = 0.60(0.61)$ for $\Lambda = 0.5(1.0)$ GeV; the T -matrix has a bound/virtual (depending on the cutoff) Z_{cs}

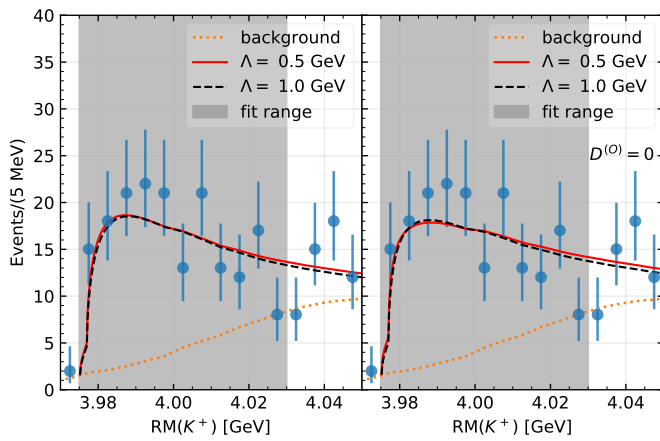


FIG. 3. Fits to the BESIII event-spectrum for a c.m. e^+e^- energy of 4.681 GeV [3], as a function of $RM(K^+) = \sqrt{(p_{e^-} + p_{e^+} - p_{K^+})^2}$. Left: best-fit results with both $C^{(O)}$ and $D^{(O)}$ taken as free parameters. Right: best-fit results within the constant-contact EFT, i.e., $D^{(O)} = 0$. The background contribution, in both plots, is taken as the combined background in the BESIII analysis.

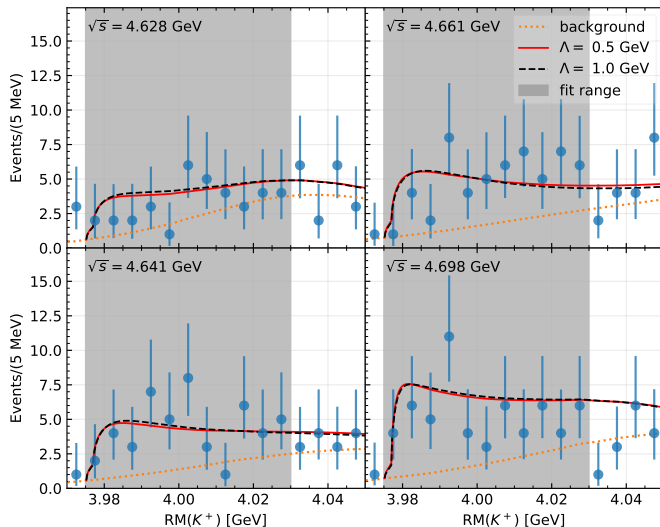


FIG. 4. Best-fit results, with both $C^{(O)}$ and $D^{(O)}$ taken as free parameters, for the event-spectra reported by BESIII for another four c.m. e^+e^- energies [3].

close to threshold. For the resonant EFT, we determine

$$\begin{aligned} C^{(O)}(\Lambda) &= -0.72^{+0.18}_{-0.13} \left(-0.44^{+0.06}_{-0.05} \right) \text{fm}^2, \\ D^{(O)}(\Lambda) &= -0.17^{+0.21}_{-0.21} \left(-0.025^{+0.066}_{-0.049} \right) \text{fm}^4, \end{aligned} \quad (20)$$

with $\chi^2/\text{dof} = 0.60(0.61)$, and consequently the Z_{cs} turns out to be a resonance. The pole position of the Z_{cs} and its spin and SU(3)-flavor partners, using these parameters, are summarized in the lower half of Table I. Although the central values of the poles differ from those using the $Z_c(3900)$ inputs, they agree within uncertainties.

A comparison of these fits with the data is shown in

Fig. 3 for the e^+e^- c.m. energy 4.681 GeV. One sees that there is no prominent narrow peak though the near-threshold enhancement is still evident. The two cases, constant-contact and resonant EFT, can both fit the data well. This is similar to the case of the $Z_c(3900)$ in the analysis of Ref. [19]. Therefore, to distinguish the two scenarios, further experimental exploration with more statistics would be helpful. The comparison for the other four energy points is shown in Fig. 4 with the resonant EFT fit. From the figure, we can see that the fit also describes the four recoil-mass spectra well simultaneously.

Summary and outlook.—We have investigated the newly observed charged hidden-charm state $Z_{cs}(3985)$ by BESIII in the processes $e^+e^- \rightarrow K^+(D_s^- D^{*0} + D_s^{*-} D^0)$. We present the first theoretical fit to all energy points, for which we consider two different EFTs describing the Z_{cs} . Three findings are worth noticing: First, the mass of this state does not necessarily coincide with that from the parametrization, and the Z_{cs} could be either a virtual state or a resonance. Second, the near-threshold signal is further enhanced when the e^+e^- energy is close to the $D_{s2}\bar{D}_s^*$ threshold at 4.681 GeV. Third, the Z_{cs} is probably the SU(3)-flavor partner of the previously known $Z_c(3900)$, which also implies the existence of a so far unobserved Z_{cs}^* state as its spin partner.

The poles presented here correspond to an isospin triplet (Z_c^\pm, Z_c^0) and two isospin doublets (Z_{cs}^+, Z_{cs}^0 and their antiparticles), as well as their spin partners. In the whole SU(3)-flavor multiplet family containing a singlet and an octet, there should be two more isospin scalars. The physical isoscalar states should be mixtures of the octet isoscalar and the singlet, the prediction of which requires more inputs.

Future experiments would be required to establish the SU(3) and spin multiplets. High statistics data for the $e^+e^- \rightarrow J/\psi K\bar{K}$ at similar energies are desirable.

ACKNOWLEDGMENTS

This work is partly supported by the National Natural Science Foundation of China (NSFC) under Grants No. 11735003, No. 11835015, No. 11947302, No. 11975041, No. 11961141012, No. U2032109, and No. 11621131001 (the Sino-German Collaborative Research Center CRC110 ‘‘Symmetries and the Emergence of Structure in QCD’’), by the Fundamental Research Funds for the Central Universities, by the Chinese Academy of Sciences (CAS) under Grants No. XDB34030303 and No. QYZDB-SSW-SYS013, by the CAS Center for Excellence in Particle Physics (CCEPP), by the Spanish Ministerio de Economía y Competitividad (MINECO) and the European Regional Development Fund (ERDF) under contract FIS2017-84038-C2-1-P, by the EU Horizon 2020 research and inno-

vation programme, STRONG-2020 project, under grant agreement No. 824093, by Generalitat Valenciana under contract PROMETEO/2020/023, and by the CAS President's International Fellowship Initiative (PIFI) under Grant No. 2020VMA0024.

APPENDIX: DETAILS OF THE FIT

The $\bar{D}_s^* D^0 + \bar{D}_s D^{*0}$ invariant mass distribution from the diagrams shown in Fig. 1 is given by

$$\frac{d\Gamma}{dm_{23}} = \frac{\mathcal{N} q_K p_3^*}{\sqrt{s}} \left\{ \frac{1}{2} \int_{-1}^1 d \cos \theta_3^* \left| q_K^2 \left[\frac{2m_{D_{s2}}}{m_{13}^2 - m_{D_{s2}}^2 + im_{D_{s2}} \Gamma_{D_{s2}}} + I(q_K) T_D \right] + r \left[1 + (I_{0, \bar{D}_s^* D^0} T_D - I_{0, \bar{D}_s D^{*0}} T_E) \right] \right|^2 \right. \\ \left. + \left| q_K^2 I(q_K) T_E - r \left[1 + (I_{0, \bar{D}_s^* D^0} T_D - I_{0, \bar{D}_s D^{*0}} T_E) \right] \right|^2 \right\}, \quad (21)$$

where $\mathcal{N} = \frac{m_{D_s^*} m_{D^0}}{18\pi^3} g^2$ is an overall constant, T_D and T_E are the T -matrix elements for $\bar{D}_s^* D^0 \rightarrow \bar{D}_s^* D^0$ and $\bar{D}_s^* D^0 \rightarrow \bar{D}_s D^{*0}$, respectively, r is a parameter describing the relative weight between diagrams (d,e) and diagrams (a,b,c) in Fig. 1, I_0 is the two-point nonrelativistic loop integral given by Eq. (15), and the scalar 3-point loop integral is given by [23, 28, 29]

$$I = \frac{\mu_{12} \mu_{23}}{2\pi \sqrt{a}} \left[\arctan \left(\frac{c_2 - c_1}{2\sqrt{a}(c_1 - i\epsilon)} \right) - \arctan \left(\frac{c_2 - c_1 - 2a}{2\sqrt{a}(c_2 - a - i\epsilon)} \right) \right], \quad (22)$$

where μ_{12} and μ_{23} are the reduced masses of the $D_{s2} \bar{D}_s^*$ and $\bar{D}_s^* D^0$, respectively, $a = (\mu_{23} q_K / m_{D^0})^2$, $c_1 = 2\mu_{12} b_{12}$, $c_2 = 2\mu_{23} b_{23} + q_K^2 \mu_{23} / m_{D^0}$ with $b_{12} = m_{D_{s2}} + m_{\bar{D}_s^*} - \sqrt{s}$ and $b_{23} = m_{\bar{D}_s^*} + m_{D^0} + E_K - \sqrt{s}$, and $q_K (E_K)$ is the K^+ momentum (energy) in the $e^+ e^-$ c.m. frame. The involved kinematic variables are given by

$$q_K = \frac{1}{2M} \sqrt{\lambda(s, m_K^2, m_{23}^2)}, \\ m_{13}^2 = m_K^2 + m_{D^0}^2 + 2E_1^* E_3^* - 2p_1^* p_3^* \cos \theta_3^*, \\ p_1^* = \sqrt{E_1^{*2} - m_K^2}, \quad p_3^* = \frac{1}{2m_{23}} \sqrt{\lambda(m_{23}^2, m_2^2, m_3^2)}, \\ E_3^* = \frac{m_{23}^2 - m_2^2 + m_3^2}{2m_{23}}, \quad E_1^* = \frac{s - m_{23}^2 - m_K^2}{2m_{23}}. \quad (23)$$

For the process with the $K^+ \bar{D}_s^* D^0$ final state, $m_2 = m_{D_s^*}$ and $m_3 = m_{D^0}$; for that with the $K^+ \bar{D}_s D^{*0}$ final state, $m_2 = m_{D_s}$ and $m_3 = m_{D^{*0}}$. To a very good approximation, p_3^* for the two processes can be taken to be the same, leading to the above expression. With the single-channel approximation, we also have $T_D = -T_E = \tau(E_{\text{cm}})/2$ with $\tau(E_{\text{cm}})$ given by Eq. (14).

In the fit, we assume that the parameter r is the same for each energy point. While for the production of the

process $e^+ e^- \rightarrow K^+ (D_s^- D^{*0} + D_s^{*-} D^0)$, we have

$$\frac{dN}{dm_{23}} = h \left| \frac{2m_\psi}{s - m_\psi^2 + im_\psi \Gamma_\psi} \right|^2 \frac{d\Gamma}{dm_{23}} \mathcal{L}_{\text{int}} \bar{\epsilon} f_{\text{corr}} \quad (24)$$

where ψ is the charmonium $\psi(4660)$. \mathcal{L}_{int} , $\bar{\epsilon}$ and f_{corr} are the integrated luminosity, detection efficiency and correction factor, respectively, which can be found in the Table I of BESIII paper [4]. The factor h is associated with the $e^+ e^-$ annihilation vertex, here we take a same value at the energy range from 4.628 to 4.698 GeV. Thus, we introduce the fit parameter $\tilde{\mathcal{N}} = \mathcal{N} h$, which is independent of c.m. $e^+ e^-$ energy.

In the constant-contact EFT fit, we have 3 free parameters, $\tilde{\mathcal{N}}$, $C^{(O)}$ and r . The correlation matrices for $\Lambda = 0.5$ GeV and $\Lambda = 1$ GeV are

$$\begin{pmatrix} 1.0 & 0.15 & 0.81 \\ 0.15 & 1.0 & -0.28 \\ 0.81 & -0.28 & 1.0 \end{pmatrix} \quad (25)$$

and

$$\begin{pmatrix} 1.0 & 0.1 & 0.82 \\ 0.1 & 1.0 & -0.34 \\ 0.82 & -0.34 & 1.0 \end{pmatrix}, \quad (26)$$

respectively. While in the resonant EFT fit, we have 4 free parameters, $\tilde{\mathcal{N}}$, $C^{(O)}$, $D^{(O)}$ and r . The correlation matrices for $\Lambda = 0.5$ GeV and $\Lambda = 1$ GeV are

$$\begin{pmatrix} 1.0 & 0 & -0.04 & 0.85 \\ 0 & 1.0 & -0.58 & -0.2 \\ -0.04 & -0.58 & 1.0 & -0.13 \\ 0.85 & -0.2 & -0.13 & 1.0 \end{pmatrix} \quad (27)$$

and

$$\begin{pmatrix} 1.0 & 0.09 & -0.07 & 0.85 \\ 0.09 & 1.0 & -0.67 & -0.16 \\ -0.07 & -0.67 & 1.0 & -0.07 \\ 0.85 & -0.16 & -0.07 & 1.0 \end{pmatrix}, \quad (28)$$

respectively.

* zhiyang@uestc.edu.cn

† caoxu@impcas.ac.cn

‡ fkguo@itp.ac.cn

§ jmnieves@ific.uv.es

¶ mpavon@buaa.edu.cn

- [1] C. Shen *et al.* (Belle), *Phys. Rev. D* **89**, 072015 (2014), [arXiv:1402.6578 \[hep-ex\]](#).
- [2] C. Yuan *et al.* (Belle), *Phys. Rev. D* **77**, 011105 (2008), [arXiv:0709.2565 \[hep-ex\]](#).
- [3] M. Ablikim *et al.* (BESIII), *Phys. Rev. D* **97**, 071101 (2018), [arXiv:1802.01216 \[hep-ex\]](#).
- [4] M. Ablikim *et al.* (BESIII), (2020), [arXiv:2011.07855 \[hep-ex\]](#).
- [5] S. H. Lee, M. Nielsen, and U. Wiedner, *J. Korean Phys. Soc.* **55**, 424 (2009), [arXiv:0803.1168 \[hep-ph\]](#).
- [6] M. B. Voloshin, *Phys. Lett.* **B798**, 135022 (2019), [arXiv:1901.01936 \[hep-ph\]](#).
- [7] J. Ferretti and E. Santopinto, *JHEP* **04**, 119 (2020), [arXiv:2001.01067 \[hep-ph\]](#).
- [8] D.-Y. Chen, X. Liu, and T. Matsuki, *Phys. Rev. Lett.* **110**, 232001 (2013), [arXiv:1303.6842 \[hep-ph\]](#).
- [9] M. Ablikim *et al.* (BESIII), *Phys. Rev. Lett.* **110**, 252001 (2013), [arXiv:1303.5949 \[hep-ex\]](#).
- [10] M. Ablikim *et al.* (BESIII), *Phys. Rev. Lett.* **111**, 242001 (2013), [arXiv:1309.1896 \[hep-ex\]](#).
- [11] P. Zyla *et al.* (Particle Data Group), *PTEP* **2020**, 083C01 (2020).
- [12] A. Bondar *et al.* (Belle), *Phys. Rev. Lett.* **108**, 122001 (2012), [arXiv:1110.2251 \[hep-ex\]](#).
- [13] M. Voloshin, *Phys. Rev. D* **93**, 074011 (2016), [arXiv:1601.02540 \[hep-ph\]](#).
- [14] F.-K. Guo, C. Hidalgo-Duque, J. Nieves, and M. P. Valderrama, *Phys. Rev.* **D88**, 054007 (2013), [arXiv:1303.6608 \[hep-ph\]](#).
- [15] V. Baru, E. Epelbaum, J. Gegelia, C. Hanhart, U. Meißner, and A. Nefediev, *Eur. Phys. J. C* **79**, 46 (2019), [arXiv:1810.06921 \[hep-ph\]](#).
- [16] C. Hidalgo-Duque, J. Nieves, and M. P. Valderrama, *Phys. Rev.* **D87**, 076006 (2013), [arXiv:1210.5431 \[hep-ph\]](#).
- [17] F.-Z. Peng, M.-Z. Liu, Y.-W. Pan, M. Sánchez Sánchez, and M. Pavon Valderrama, (2019), [arXiv:1907.05322 \[hep-ph\]](#).
- [18] M. P. Valderrama, *Phys. Rev.* **D85**, 114037 (2012), [arXiv:1204.2400 \[hep-ph\]](#).
- [19] M. Albaladejo, F.-K. Guo, C. Hidalgo-Duque, and J. Nieves, *Phys. Lett. B* **755**, 337 (2016), [arXiv:1512.03638 \[hep-ph\]](#).
- [20] L. Landau, *Nucl. Phys.* **13**, 181 (1960).
- [21] S. Coleman and R. Norton, *Nuovo Cim.* **38**, 438 (1965).
- [22] F.-K. Guo, X.-H. Liu, and S. Sakai, *Prog. Part. Nucl. Phys.* **112**, 103757 (2020), [arXiv:1912.07030 \[hep-ph\]](#).
- [23] F.-K. Guo, C. Hanhart, U.-G. Meißner, Q. Wang, Q. Zhao, and B.-S. Zou, *Rev. Mod. Phys.* **90**, 015004 (2018), [arXiv:1705.00141 \[hep-ph\]](#).
- [24] Q. Wang, C. Hanhart, and Q. Zhao, *Phys. Rev. Lett.* **111**, 132003 (2013), [arXiv:1303.6355 \[hep-ph\]](#).
- [25] Q. Wang, C. Hanhart, and Q. Zhao, *Phys. Lett.* **B725**, 106 (2013), [arXiv:1305.1997 \[hep-ph\]](#).
- [26] X.-H. Liu, *Phys. Rev.* **D90**, 074004 (2014), [arXiv:1403.2818 \[hep-ph\]](#).
- [27] A. Pilloni, C. Fernandez-Ramirez, A. Jackura, V. Mathieu, M. Mikhasenko, J. Nys, and A. P. Szczepaniak (JPAC), *Phys. Lett.* **B772**, 200 (2017), [arXiv:1612.06490 \[hep-ph\]](#).
- [28] F.-K. Guo, (2020), [arXiv:2001.05884 \[hep-ph\]](#).
- [29] F.-K. Guo, C. Hanhart, G. Li, U.-G. Meißner, and Q. Zhao, *Phys. Rev. D* **83**, 034013 (2011), [arXiv:1008.3632 \[hep-ph\]](#).
- [30] F. James and M. Roos, *Comput. Phys. Commun.* **10**, 343 (1975).
- [31] iminuit team, “iminuit: A Python interface to MINUIT,” <https://github.com/scikit-hep/iminuit>.
- [32] F.-K. Guo, “IMinuit.jl: A Julia wrapper of iminuit,” <https://github.com/fkguo/IMinuit.jl>.